

## UV-LASER-INDUCED PHOTODESORPTION OF NO FROM NiO

P.M. FERM \*, F. BUDDE \*\*, A.V. HAMZA \*\*\*, S. JAKUBITH,  
G. ERTL

*Fritz-Haber-Institut der Max-Planck-Gesellschaft, 1000 Berlin 33, Germany*

D. WEIDE, P. ANDRESEN

*Max-Planck-Institut für Strömungsforschung, 3400 Göttingen, Fed. Rep. of Germany*

and

H.J. FREUND

*Institut für Physikalische Chemie, Ruhr-Universität, 4630 Bochum, Fed. Rep. of Germany*

Received 21 December 1988; accepted for publication 7 April 1989

Irradiation of a NO covered NiO surface by UV photons ( $h\nu = 5.0$  and  $6.4$  eV, respectively) yields desorption with a quantum yield of the order  $10^{-2}$ . Fully state-resolved determination of the energy distributions of the desorbing particles were performed by means of laser-induced fluorescence and demonstrated the non-thermal origin of at least part of them. Bimodal velocity distributions, a pronounced spin-orbit selectivity for molecules with low rotational levels, and an increase of the mean translational energy with increasing rotational energy are the most remarkable effects observed. The results are qualitatively discussed on the basis of current concepts for desorption via electronic excitation and for scattering of open-shell molecules at surfaces.

### 1. Introduction

Processes such as laser-induced chemical vapour deposition, laser etching or laser ablation are of growing interest with respect to application in microelectronics [1–5] and comprise the variation of the chemical state of a surface by irradiation with laser light. In many of these laser-assisted processes, thermal and non-thermal (i.e. photochemical) pathways are conceivable, but mostly the exact mechanisms are still unknown.

\* Present address: Allied-Signal Inc., Engineered Materials Research, Morristown, NJ 07960, USA.

\*\* Present address: IBM Thomas J. Watson Research Center, Yorktown Heights, NY 10598, USA.

\*\*\* Present address: Sandia National Laboratories, Surface Science and Chemical Physics Division, Livermore, CA 94550, USA.

Laser-induced desorption is probably the conceptually simplest process in this class of surface reactions and has already been studied under different aspects. The substrate–adsorbate bond can either be broken from the electronic ground state of the system by vibrational excitation, or – if the photon energy is high enough – through intermediate electronic excitation. In the UV spectral region ( $h\nu < 10$  eV), light absorption leads to excitations of electrons in the valence levels, either within the substrate, the adsorbate, or the substrate–adsorbate bond. This electronic excitation energy can either relax into the heat bath of the solid so that the net result might be thermal desorption due to the associated temperature rise, or it can be converted into translational motion of the adsorbate away from the surface before complete thermalization has occurred. This latter channel bears close similarities to electron-stimulated desorption, and therefore both processes are classified as desorption induced by electronic transitions (DIET) [6]. Evidence for the operation of such non-thermal desorption channels after irradiation with UV laser radiation has already been reported for a number of systems [7–20].

The dynamics of thermal desorption as well as the scattering of molecules in their ground state interaction potential with the surface could already be investigated in great detail by the combination of molecular beam and laser spectroscopic techniques [21]. In this way information about the translational energy distributions of molecules coming off the surface in individual internal quantum states, as well as about the relative populations of the latter becomes experimentally accessible [22]. Application of these methods to systems undergoing photon-excited desorption is expected to provide insight into the dynamics of these processes which is still a widely unknown area.

In this paper we report on the results of fully state-resolved measurements (i.e. with respect to translational, rotational, vibrational, and spin–orbit energy distributions) for NO desorbing from a NiO surface upon irradiation with ArF or KrF-excimer laser light ( $h\nu = 6.4$  and  $5.0$  eV, respectively). By considering the balance of total energy in this way, the amount of energy exchanged with the solid becomes also experimentally accessible. Preliminary previous results [19] suffered from insufficient surface characterization, while a brief report of some of the present findings was published recently [20].

## 2. Experimental

The apparatus used in this study was a standard UHV system (base pressure below  $7 \times 10^{-10}$  Torr) which was equipped with a molecular beam, a rotatable quadrupole mass spectrometer for residual gas analysis and thermal desorption spectroscopy (TDS), and with facilities for low energy electron diffraction (LEED), Auger electron spectroscopy (AES), and argon ion bombardment.

The orientation of the (100) plane of the Ni sample was controlled by Laue diffraction to be within  $0.5^\circ$  of the surface normal. The sample was mounted between a pair of Ni wires and could be radiatively heated. Temperature was measured by a chromel–alumel thermocouple spot-welded on the rear of the crystal. Cooling was achieved by means of thermal contact of the crystal holder to a liquid nitrogen reservoir. The lowest temperature reached this way was about 140 K which was also the standard surface temperature,  $T_s$ , used. The sample surface was cleaned according to a procedure described by Koel et al. [23]: 3 min of  $\text{Ar}^+$  bombardment at 500 K, 2 min of  $\text{Ar}^+$  bombardment at 800 K and 30 min annealing at 750 K were followed by an oxidation–reduction cycle (flashing to 800 K in  $2 \times 10^{-7}$  torr  $\text{O}_2$ ; 10 min in  $2 \times 10^{-7}$  Torr  $\text{H}_2$  at 750 K). The oxidation–reduction cycle was repeated until no impurities were detectable by AES. The degree of surface order was checked by LEED. Some measurements were carried out with a pre-oxidized surface which was obtained by dosing 300–400 L oxygen at  $T_s = 400$  K.

The desorption was initiated by an excimer laser (Lambda Physik EMG 200) which was run either in ArF ( $\lambda = 193$  nm,  $h\nu = 6.4$  eV) or KrF ( $\lambda = 248$  nm,  $h\nu = 5.0$  eV) mode with a pulse duration of 15 ns (FWHM). Using a diaphragm a beam of 10 mm diameter was created and directed onto the sample. Typically, the fluence was  $2.5$  mJ/cm<sup>2</sup> per pulse and the repetition rate was set at 10 Hz. Under these conditions, the calculated raise of the surface temperature during the laser pulse is smaller than 20 K [24].

Desorbing NO molecules were probed by laser-induced fluorescence (LIF) via the  $\text{A}^2\Sigma^+(v', J') \leftarrow \text{X}^2\Pi(v'', J'')$  absorption band at 226 nm. For this purpose the frequency-doubled light of an excimer pumped dye laser was used (Lambda Physik EMG 201 E and Lambda Physik FL 2002). The pulse duration of this system was 12 ns before and 8 ns after frequency doubling. The band width of this laser system is  $0.18$  cm<sup>-1</sup>. At the point of detection the beam has a diameter of 4 mm (FWHM). The pulse energy was reduced to typically  $15$   $\mu\text{J}$ /pulse. The dependence of the LIF-signal intensity on the probe laser energy was linear in the range from 0 to 130  $\mu\text{J}$ , well below saturation. The probe laser intersects the desorbing molecules parallel to the Ni surface and perpendicular to the plane formed by the desorption laser and molecular beams. In the standard geometry used, the desorption laser was directed normal to the surface while the detection angle and the angle of incidence of the molecular beam were  $45^\circ$  and  $45^\circ$  with respect to the surface normal. The angle of incidence of the desorption laser beam and the detection angle could be varied by rotating the sample. However, the angle between the desorption laser beam and the direction of detection remained fixed at  $45^\circ$ . The distance between the probe laser beam and the surface (identical with the flight distance of the desorbing particles) could be varied between 14 and 40 mm and was set typically at 25 mm. It should be remembered that rather the particle density than the flux is measured with LIF.

State-selective time-of-flight (TOF) measurements were performed by variation of the delay between the desorption and the probe laser shot with the probe laser tuned to a specific absorption line, thus selecting the quantum state under investigation. The diameter of the probe laser beam (about 3 mm) and the imaging optics determine the detection volume which limits – together with the spatial extension of the sample – the velocity resolution to about  $\Delta V/V \approx \pm 0.1$ . Rotational state distributions were obtained by scanning the wavelength of the probe laser at a fixed time delay between desorption and probe laser. In cases where the TOF distributions were different in varying rotational states, these distributions were integrated by changing the time delay while taking data points at the same probe laser wavelength. Data acquisition of TOF spectra as well as of rotational state distribution was controlled by a micro-computer.

Suppression of stray light of the desorption laser was achieved in different ways: First, a gated photomultiplier (PMT) was used for the detection of the laser-induced fluorescence: the voltage between the cathode and the first dynode of the PMT is only turned on after the desorbing laser had been fired. Second, two reflection filters (Schott UV-R-250) were mounted in the front of the PMT with maximum transmittance at 250 nm. The selective transmission results in a changing detection efficiency which had to be considered when extracting relative populations in different vibrational states (i.e.  $(v'' = 0)/(v'' = 1) = 2.3$ , this value also cares for the different Franck–Condon factors of absorption and emission for the (0, 0) and the (1, 1) bands probed). Finally, also in order to reduce scattered stray light from the desorption laser, the sample mounting was covered with graphite.

The surface could be dosed either with a molecular beam (a pure NO beam was used with a calculated translational energy of 90 meV and a measured rotational temperature of 40 K) or by rising the NO background pressure. In case of dosing with the molecular beam, the background signal caused by the molecules scattered from the surface was smaller than 5% of the desorption signal and could be neglected. This was not possible in the case of dosing with background pressure. In order to discriminate between background and desorbing molecules, the desorption laser was fired at 5 Hz, whereas the probe laser was operated at 10 Hz. With every pulse either the signal  $I_1$  of the residual NO or the signal  $I_2$  corresponding to both residual NO and laser-desorbed NO is measured. A boxcar integrator is used to obtain the difference of the two signals ( $I_2 - I_1$ ) which is equivalent to the desorption signal.

The procedures for the quantitative analysis of the TOF spectra have already been described previously [25]. In brief, the spectra reflected the density of desorbing particles fitted with a non-linear least-squares fitting routine using a modified Maxwell–Boltzmann distribution  $N(t) = at^{-3} \exp[-b(d/t - v_0)^2]$ , where  $a$  is a normalization factor,  $v_0$  is a flow velocity,  $d$  is the surface-to-detector distance and  $b$  is a measure of the

distribution width. In the case of a Maxwell–Boltzmann distribution  $v_0 = 0$  and  $b = m/2kT$ . TOF spectra showing two peaks were fitted with a pair of such functions. The mean translational energy  $\langle E_{\text{trans}} \rangle$ , the mean velocity  $\langle v \rangle$  and the mean variance  $\langle \sigma^2 \rangle$  can be derived by numerical intergration either directly from the spectra or from the fit curves [25]. Conversion of the recorded TOF spectra into velocity distributions is straightforward. The stated equation then transforms into  $f(v) = Av^2 \exp[-B(v - v_0)^2]$ . For the calculation of rotational state distributions, the relative population of an individual rotational level is obtained by dividing the peak height of the corresponding LIF line by the Hönl–London factor [26]. If the distribution can be described by Boltzmann statistics, then  $N_{J''} \propto (2J'' + 1) \exp(-E_{\text{int}}/kT_{\text{rot}})$ , where  $E_{\text{int}} = E_{\text{el}} + E_{\text{rot}}$ , and a plot of  $\ln[N_{J''}/(2J'' + 1)]$  versus  $E_{\text{int}}$  (“Boltzmann plot”) yields a straight line whose slope is determined by the rotational temperature  $T_{\text{rot}}$ .  $E_{\text{el}}$  accounts for the fact that two different electronic states of the NO molecule are probed ( ${}^2\Pi_{1/2}$  and  ${}^2\Pi_{3/2}$ ), separated by  $\Delta E_{\text{el}} = 123.18 \text{ cm}^{-1}$  [27]. This refers to molecules in the vibrational ground state ( $v'' = 0$ ); otherwise the vibrational energy has to be included.

### 3. Results

#### 3.1. Laser-induced transformation of the surface

Experiments on the laser-induced desorption of NO were typically performed in the following way: The surface held at 140 K was exposed to a steady-state flux of NO molecules (either from the molecular beam or from the background of the chamber adjusted to a certain partial pressure) and then the desorption laser was switched on with a given repetition frequency and pulse power. Between two successive laser shots the desorbed molecules could be replaced by readsorption from the gas phase, so that rapid (i.e. after the first few laser pulses) establishment of the steady-state surface concentration of adsorbed NO molecules was to be expected. Detection of the molecules desorbed by the laser pulse can most conveniently be achieved by tuning the probe laser to an intense transition and firing it after an appropriately chosen delay time.

Fig. 1 shows the variation of the concentration of desorbing NO molecules, as probed via the population of the  $J'' = 5/2$  state at a fixed delay time, with the number of desorption laser pulses (ArF, 3 mJ/pulse) after exposing a *clean* Ni(100) surface at 140 K to a NO atmosphere of  $5 \times 10^{-7}$  Torr. The intensity decays during the first few shots and then, surprisingly, increases continuously until it reaches a steady-state value after about 3000–5000 pulses, i.e. 10–20 min. Such a long time for reaching steady-state cannot be reconciled with a simple adsorption–desorption mechanism, but has to be

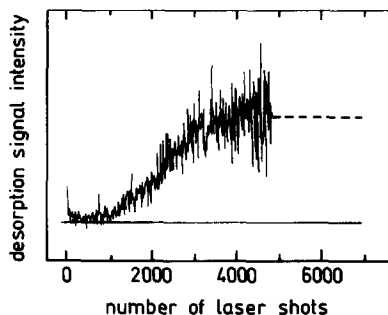


Fig. 1. Variation of the intensity of the NO desorption signal with the number of laser shots ( $h\nu = 6.4$  eV) if a clean Ni(100) surface at 140 K is exposed to a constant steady-state NO gas flux.

attributed to an irreversible variation of the state of the surface. After termination of the desorption experiment Auger spectroscopy revealed the presence of substantial amounts of oxygen (but only of traces of nitrogen) on the surface, thus suggesting the transformation of the metallic surface into an oxidized one which exhibits a considerably higher cross section for laser-induced desorption of adsorbed NO.

This suggestion was confirmed by a series of thermal desorption spectroscopy (TDS) experiments: Curve (a) of fig. 2 is the NO thermal desorption spectrum from a Ni(100) surface which had been saturated with adsorbed NO at 140 K. It is in full agreement with the data reported by Peebles et al. [28] for the same system and consists of a peak at 345 K with a shoulder at 380 K. Curve (b) was recorded after prolonged laser irradiation and subsequent post-exposure to NO prior to thermal desorption. Obviously a new low-temperature state with its maximum at 220 K has been created by the laser interaction. It is just this state which exhibits a high yield for photodesorption: If after reaching the steady-state the NO flux is switched off while laser irradiation continues, the photodesorption signal decays continuously and a subsequent TDS experiment (curve (c)) shows that it is just the new low-temperature state which was most efficiently depopulated. If the Ni(100) surface is pre-oxidized by interaction with O<sub>2</sub> and subsequently exposed to NO, TDS exhibits mainly the low temperature state while the desorption states above 300 K from metallic Ni are practically absent (d).

Interaction of O<sub>2</sub> with clean Ni surfaces is known to lead (via intermediate chemisorbed phases) to the growth of epitaxial layers of NiO exhibiting a band gap [29]. Recent ARUPS/HREELS studies indicate that NO is adsorbed on such a surface with its molecular axis normal to the surface plane, as will be described in detail elsewhere [30].

The transformation of an NO covered Ni(100) surface into NiO under the influence of UV laser irradiation is most probably not due to photodissocia-

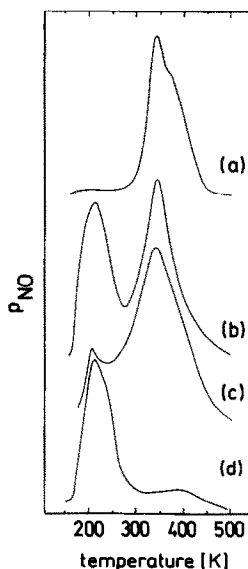


Fig. 2. Series of thermal desorption spectra for NO: (a) after exposing a clean Ni(100) to NO; (b) a NO covered Ni(100) surface was subject to prolonged UV laser irradiation and had subsequently again be exposed to NO; (c) as before, but without redosing of NO; (d) the Ni(100) surface was pre-oxidized by O<sub>2</sub> and subsequently exposed to NO.

tion of adsorbed NO, but of adsorbed NO<sub>2</sub> ( $\rightarrow$  NO + O) which was found to be present as a low-concentration impurity in the gas used. This conclusion is based on observations made in a current study on the photodecomposition of NO<sub>2</sub> adsorbed on Pd(111) [31], and explains also the absence of N atoms on the surface. The rather slow transformation of the surface into its steady-state as reflected by the data of fig. 1 is due to the fact that the low partial pressure of NO<sub>2</sub> ( $< 10^{-8}$  Torr) requires large exposure times for the completion of the NiO overlayer.

To summarize this section: All photodesorption experiments to be described in the following concern NO adsorbed on a NiO surface, whereby no difference exists between surfaces prepared by pre-oxidation of metallic Ni or formed by laser-induced decomposition of NO<sub>2</sub> adsorbed on Ni(100). This NO species desorbs thermally around 220 K, from which an adsorption energy of about 13 kcal/mol is estimated.

### 3.2. Desorption yields

If the NiO surface (area  $\sim 1$  cm<sup>2</sup>) is saturated with NO at 140 K and then irradiated – without redosing from the gas phase – with about  $2.4 \times 10^{15}$  photons ( $h\nu = 6.4$  eV) per laser pulse, about 100 shots are needed in order to

depopulate the adlayer. On the basis of data about the NO saturation coverage on NiO [32] we estimate that this corresponds to the desorption of about  $4 \times 10^{14}$  molecules/cm<sup>2</sup>. From a simple calculation the quantum yield results to be of the order of  $10^{-2}$  and the cross section for desorption to be about  $2 \times 10^{-17}$  cm<sup>2</sup>. If one takes the pulse duration into account, one obtains for the flux of desorbing molecules a value of about  $1.2 \times 10^{21}$  particles/s. The volume into which the desorbing molecules are confined during the laser shot is about  $2 \times 10^{-3}$  cm<sup>3</sup>, if a mean velocity of  $10^3$  m/s is assumed, from which a density corresponding to a pressure of about 0.3 Torr results. The mean free path at this pressure is of the order of 0.5 mm, which is still considerably larger than the distance of  $2 \times 10^{-2}$  mm which is traversed by the molecules during the duration of the laser shot. At later times the density rapidly decreases and velocity segregation proceeds, making collisions less and less probable. It is therefore concluded that gas-phase collisions are negligible under the applied experimental conditions, which is of course of vital importance for interpretation of the state-resolved data to be presented below. This conclusion is also in full agreement with the findings of Cowin et al. [33] who in laser-induced thermal desorption experiments found evidence for intermolecular collisions only at much higher desorption fluxes than realized in the present study.

The value of  $2 \times 10^{-17}$  cm<sup>2</sup> given for the photodesorption cross section should be considered only as a very rough estimate of the order of magnitude, not only because of the experimental uncertainties underlying its derivation, but because it is furthermore strongly affected by the state of the adsorbate, i.e. its coverage.

The coverage under steady-state conditions will depend on the NO pressure and will continuously increase with  $p_{\text{NO}}$  until it reaches its saturation value. As can be seen from fig. 3, the desorption yield (as monitored through the intensity of the  $J'' = 5/2$  level) increases at first with increasing pressure – as

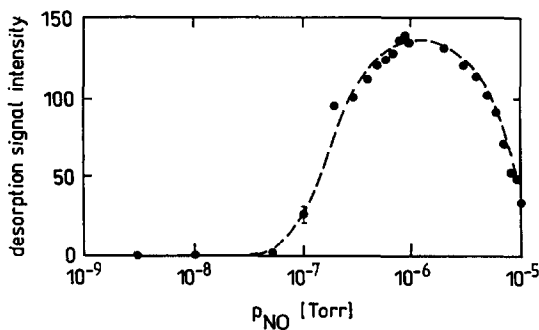


Fig. 3. Dependence of the NO photodesorption signal (as monitored through the relative population of the  $J'' = 5/2$ ,  $v'' = 0$ ,  ${}^2\Pi_{1/2}$  level) on the steady-state pressure of NO at  $T_s = 140$  K.

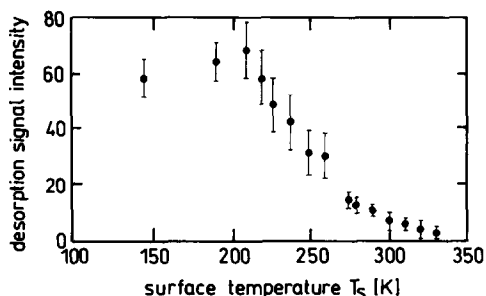


Fig. 4. Dependence of the NO photodesorption signal on surface temperature at fixed  $p_{\text{NO}} = 4 \times 10^{-7}$  Torr.

expected – but then decays again to much lower values, although the surface concentration of adsorbed NO increases. From this it has to be concluded that the photodesorption cross section for more tightly packed molecules is much smaller than for those at lower coverage, a phenomenon which is well known from electron-stimulated desorption (ESD) [34] and which can certainly not be reconciled with a thermal origin of the desorption process.

The influence of coverage is also reflected in the results of an experiment which was performed at constant  $p_{\text{NO}}$  and varying temperature instead of the isothermal conditions underlying fig. 3. As can be seen from fig. 4, the desorption drops rapidly between 200 and 250 K – just the temperature range for pronounced thermal desorption in fig. 2.

### 3.3. Energy distributions of desorbing molecules

#### 3.3.1. Translational energies

Fig. 5 shows a typical set of time-of-flight (TOF) spectra (normalized to identical maximum intensities) for NO molecules ( $v'' = 0$ ,  $\Pi_{1/2}$  state) in various rotational states  $J''$  after desorption with 6.4 eV photons. For low rotational quantum numbers these distributions are clearly bimodal, composed of a “fast” and a “slow” contribution each of which can be fitted by a curve (full line) corresponding to a velocity distribution of the form  $f(v) = Av^2 \exp[-B(v - v_0)^2]$  (see section 2). With increasing  $J''$  the fraction of “slow” molecules decreases and is no longer discernible above  $J'' \approx 33/2$ . It is tempting to identify this bimodal distribution with two desorption channels; although there exists a priori no justification for such a procedure, we will rationalize the further data analysis on the basis of such a separation. The intensities of “fast” molecules were found to obey sharper-than-cosine (about  $\cos^2\Theta$ ) distributions with respect to the angle from the surface normal, while the angular distribution of the “slow” molecules was more of the normal cosine-type.

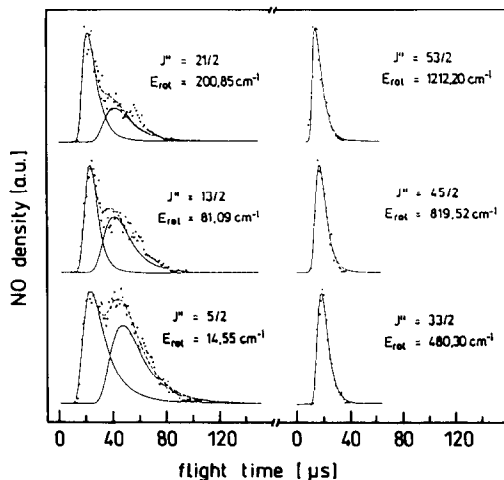


Fig. 5. Series of time-of-flight spectra for photodesorbing NO molecules ( $v'' = 0$ ,  ${}^2\Pi_{1/2}$  state) with various rotational levels  $J''$ .

Evaluation of the average translational energy as a function of the “internal” energy (i.e. the sum of rotational and spin-orbit energy) for the “fast” particles yields the data reproduced in fig. 6. Expressing the translation energy in terms of  $\langle E_{\text{trans}} \rangle / 2k$  provides a convenient basis for comparison with the surface temperature  $T_s$  and does not imply that a Maxwell-Boltzmann distribution is obeyed (in fact the observed distributions are narrower, but without exhibiting a systematic trend); for particles coming off in thermal equilibrium with the surface  $\langle E_{\text{trans}} \rangle / 2k = T_s$ . The data in fig. 6 fall onto two separate straight lines for the two different spin-orbit states,  ${}^2\Pi_{1/2}$  and  ${}^2\Pi_{3/2}$ .

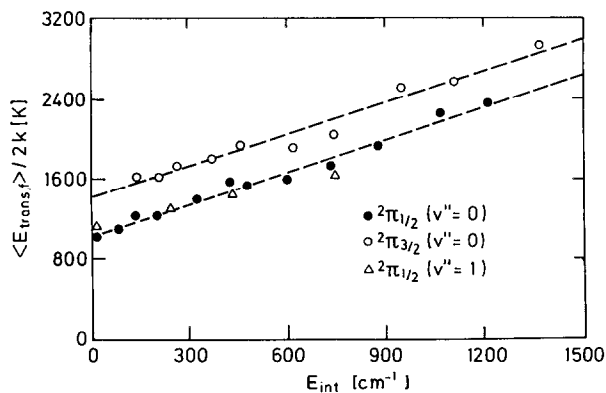


Fig. 6. Variation of the mean translational energy of desorbing “fast” molecules,  $\langle E_{\text{trans},f} \rangle$ , with their internal energy,  $E_{\text{int}}$ .

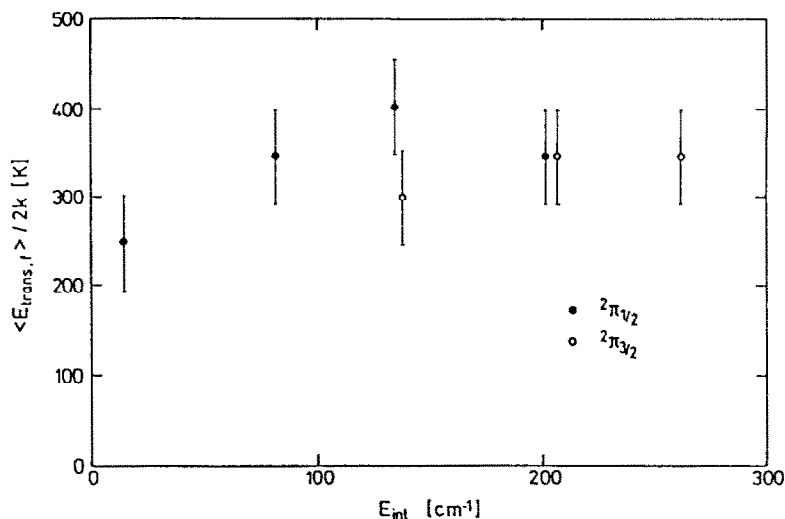


Fig. 7. Variation of the mean translational energy of desorbing “slow” particles ( $v'' = 0$ ) with their internal energy.

$\langle E_{\text{trans}} \rangle / 2k$  is much higher than  $T_s$  and increases with  $E_{\text{int}}$ ; it ranges from 1000 K ( $J'' = 5/2$ ,  ${}^2\Pi_{1/2}$ ) to 3000 K ( $J'' = 53/2$ ,  ${}^2\Pi_{3/2}$ ). At a given  $E_{\text{int}}$ ,  $\langle E_{\text{trans}} \rangle / 2k$  for  ${}^2\Pi_{3/2}$  molecules exceeds the value for the corresponding  ${}^2\Pi_{1/2}$  species by about 400 K. If instead of  $E_{\text{int}}$  the rotational energy  $E_{\text{rot}}$  would have been chosen as abscissa of fig. 6, all data for the  ${}^2\Pi_{3/2}$  particles would have been shifted by  $123.18 \text{ cm}^{-1}$  to the left. The difference in translational energy between the two spin-orbit states would then be even larger.

Corresponding data for the “slow” fraction are plotted in fig. 7. Now a value  $\langle E_{\text{trans}} \rangle / 2k = 330 \pm 50 \text{ K}$  is found. Any variation with  $E_{\text{int}}$  or the spin-orbit state is within the scatter of the data. Again the velocity distribution is narrower than a Maxwell-Boltzmann distribution of the corresponding temperature.

With the laser system used for LIF analysis of the desorbing molecules also particles with  $v'' = 1$  could be probed. Their intensity was only about 1% of those in the vibrational ground state (see below), and hence the TOF data exhibited appreciable noise levels. A typical time-of-flight spectrum is reproduced in fig. 8. The distribution is no longer bimodal but exhibits only the “fast” portion. Because of the poor signal-to-noise ratio and the overlap of many lines of the (1,1) band with those of the (0,0) band (which probes  $v'' = 0$  particles), only a limited number of levels belonging to the  ${}^2\Pi_{1/2}$  branch could be analyzed. The resulting data of  $\langle E_{\text{trans}} \rangle / k$  are included in fig. 6. There is obviously no noticeable difference with respect to the corresponding particles with  $v'' = 0$ .

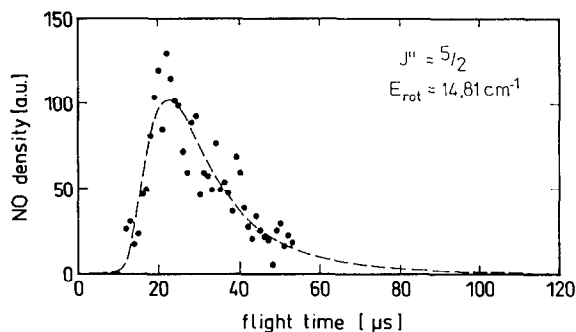


Fig. 8. Typical time-of-flight spectrum for photodesorbing molecules in the  $v'' = 1$  level.

Experiments performed with KrF laser irradiation ( $h\nu = 5.0$ ) were associated with a considerable noise level, because the filters used did not suppress scattered light from this source ( $\lambda = 248$  nm) which leads to a substantial background signal intensity.  $\langle E_{\text{trans}} \rangle$  was found to be of the same order of magnitude as that of corresponding molecules desorbed by ArF (6.4 eV) photons, but because of the large scatter of the data no more quantitative conclusions can be drawn.

### 3.3.2. Rotational and spin-orbit distributions

The relative population of “fast” molecules in a certain rotational state was derived by integrating over the corresponding TOF distribution, as outlined in the experimental section. Since perfect separation of “fast” and “slow” molecules was not feasible, the upper limit for the integration was set (somewhat arbitrarily) in the minimum between the two TOF peaks (see fig. 5). Since  $\langle E_{\text{trans}} \rangle$  for the slow particles was found to be independent of  $E_{\text{int}}$ , it sufficed in this case to record the intensity of desorbing particles at a fixed time delay between desorption and probe laser pulse. A delay corresponding to the maximum in the TOF of the slow channel was chosen. Unless otherwise stated, rotational state distributions are plotted in the usual way as “Boltzmann plots”,  $\ln[N_{J''}/(2J'' + 1)]$  versus  $E_{\text{int}}$ . In the case of a resulting straight line, from its slope a rotational temperature (a priori without any thermodynamic significance) can be formally derived.

Fig. 9 shows the resulting rotational distributions of “fast” NO molecules desorbed by 6.4 eV photons in the  $v'' = 0$  state for both the  ${}^2\Pi_{1/2}$  (a) and  ${}^2\Pi_{3/2}$  (b) branches. For the  ${}^2\Pi_{1/2}$  particles this distribution can be approximated by a straight line, yielding  $T_{\text{rot}} = 360 \pm 25$  K. This is no longer possible for the  ${}^2\Pi_{3/2}$  species which exhibit a very pronounced “underpopulation” at low rotational energies. This effect is not only evident for particles within the same spin-orbit branch (cf. fig. 9b), but becomes even more pronounced if

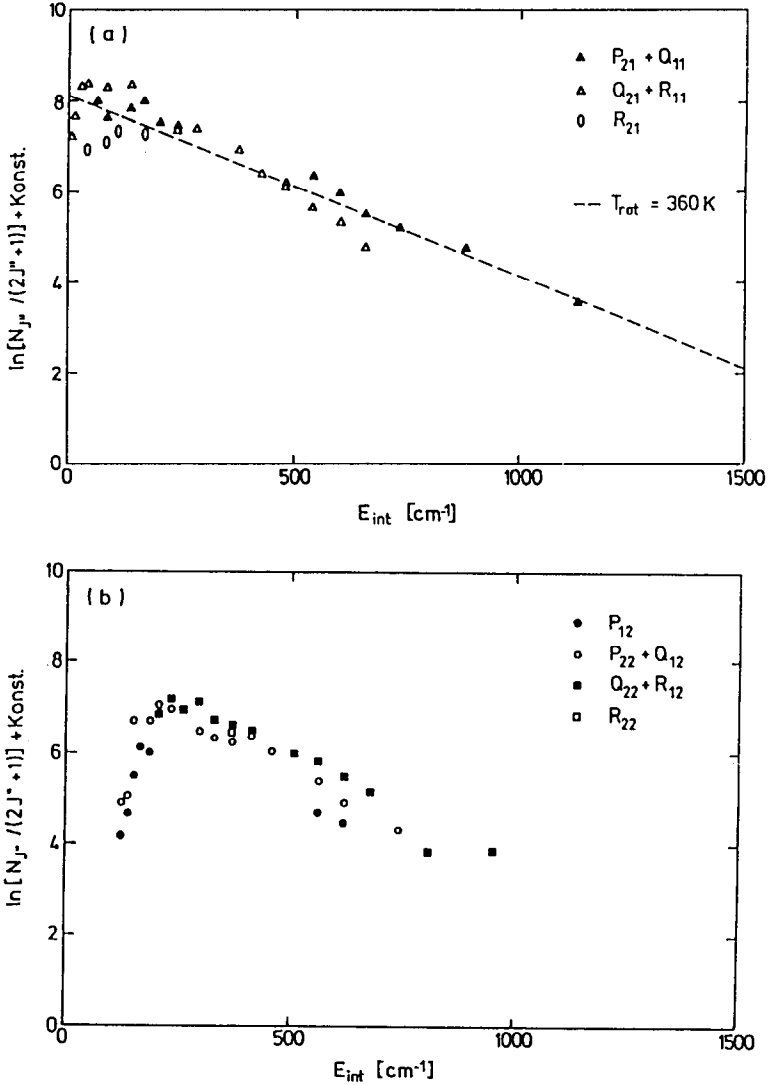


Fig. 9. "Boltzmann plots",  $\ln[N_{j''}/(2J''+1)]$  versus  $E_{\text{int}}$ , for the rotational populations of "fast" NO molecules desorbing in the  $v''=0$  level by 6.4 eV photons. The measured intensities reflecting the particle densities were converted into fluxes in order to take account of the fact that the mean velocity varies with the rotational energy: (a)  $^2\Pi_{1/2}$  manifold; (b)  $^2\Pi_{3/2}$  manifold.

molecules from both the  $^2\Pi_{3/2}$  and  $^2\Pi_{1/2}$  levels exhibiting the same rotational quantum numbers are compared with each other. Fig. 10 shows a plot of the resulting ratio of the populations as a function of  $J''$ . For the lowest rotational levels this ratio reaches values up to 40, quite in contrast to the

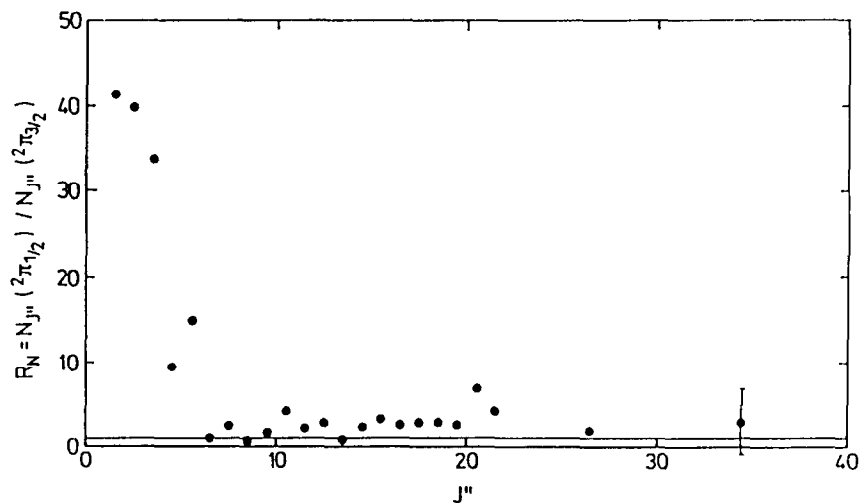


Fig. 10. Population ratio  $R_N = N_{J''}(^2\Pi_{1/2})/N_{J''}(^2\Pi_{3/2})$  of NO molecules photodesorbed by 6.4 eV photons as a function of  $J''$ .

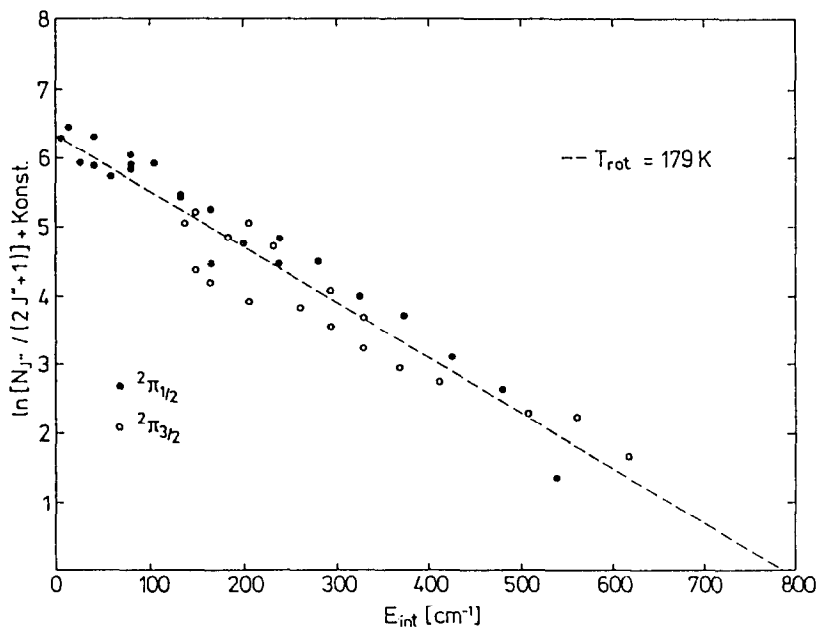


Fig. 11. "Boltzmann plot" for the rotational population of "slow" molecules desorbing by 6.4 eV photons in the  $v'' = 0$  level.

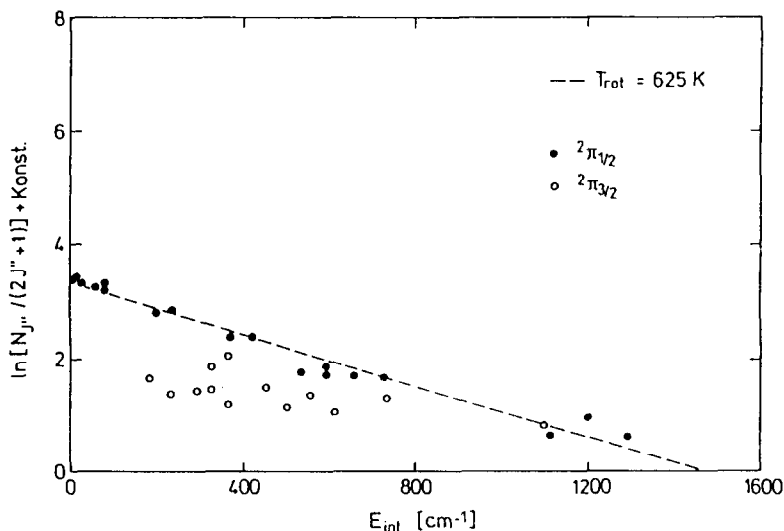


Fig. 12. "Boltzmann plot" for the rotational population of NO molecules desorbing by 6.4 eV photons in the  $v'' = 1$  level.

values close to unity usually found for molecules which were either scattered or desorbed thermally from a surface [35].

Rotational distributions for the accompanying "slow" molecules are reproduced in fig. 11. The data for the  $^2\Pi_{1/2}$  and  $^2\Pi_{3/2}$  branches fall (within the limits of error) on the same straight line corresponding to a rotational temperature of  $T_{\text{rot}} = 180 \pm 10 \text{ K}$ . The pronounced spin-orbit selectivity at low  $J''$  observed for the "fast" particles is no longer present, but instead both branches are now again equally populated. The much smaller  $T_{\text{rot}}$ , if compared with that for the "fast" molecules, is already reflected by the TOF distributions depicted in fig. 5: With increasing  $J''$  the population of the "slow" channel drops more strongly than that of the "fast" one.

Due to the small fraction of molecules desorbing in the  $v'' = 1$  state the resulting rotational populations are in this case associated with larger scatter (fig. 12). The distribution of the  $^2\Pi_{1/2}$  particles can be approximated by a straight line yielding  $T_{\text{rot}} \approx 600 \text{ K}$ . The populations of the  $^2\Pi_{3/2}$  species are systematically lower (like for the low  $J''$  molecules in the vibrational ground state), but the quality of the data is too poor to enable further conclusions.

Rotational distributions of  $v'' = 0$  molecules desorbed by KrF light ( $h\nu = 5.0 \text{ eV}$ ) are shown in fig. 13. Because of the high noise level of the data it cannot be clearly decided if at low  $J''$  the  $^2\Pi_{3/2}$  particles are gain underpopulated. The dashed line in this figure corresponds to  $T_{\text{rot}} = 350 \text{ K}$ .

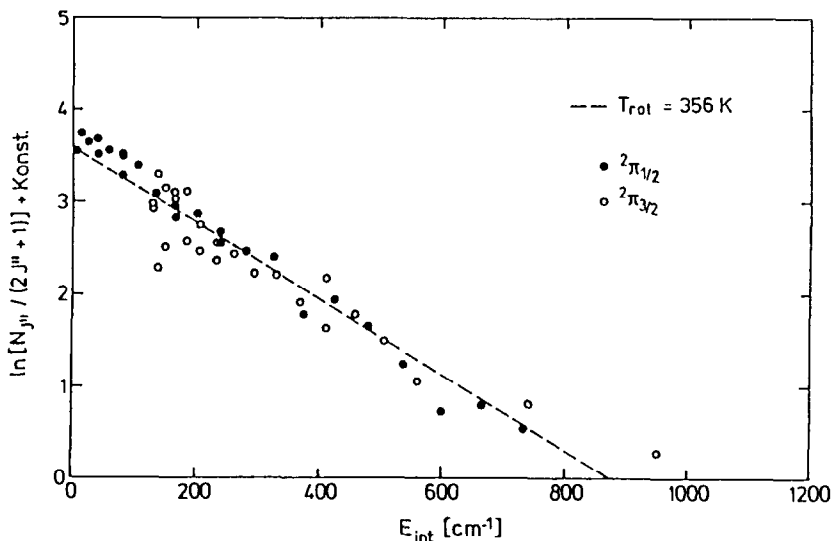


Fig. 13. "Boltzmann plot" for the rotational population of NO molecules desorbing by 5.0 eV photons in the  $v'' = 0$  level.

### 3.3.3. Vibrational energies

The population in  $v = 1$  has been estimated by comparison of signal intensities of lines in the (0, 0) and (1, 1) bands. The laser was tuned in rapid sequence to lines of same  $J$  values ( ${}^2\Pi_{1/2}$ ) belonging to both vibrational levels. About 1% of the NO molecules desorbed by 6.4 eV photons were found (under the applied experimental conditions) to be in the  $v'' = 1$  state. Assuming a Boltzmann distribution for  $N_{v''=1}/N_{v''=0}$  this would correspond to a vibrational temperature  $T_{\text{vib}} \approx 600$  K. Although the population of the  $v'' = 1$  state found in the present experiments is considerably lower than the data of the preliminary report [19] (which is probably due to the somewhat different experimental conditions), it certainly exceeds by far the numbers to be expected for thermal equilibrium with the surface. For  $T_s = 300$  K a fraction of  $10^{-4}$  and for  $T_s = 140$  K only of  $5 \times 10^{-9}$  is in the first vibrationally excited state. No information is available about the possible desorption of molecules in even higher vibrational levels.

## 4. Discussion

In discussing chemical transformations of surfaces (including desorption) caused by laser irradiation, two aspects have to be considered, namely the predominant process governing the absorption of the photons and how this energy leads to nuclear motion and bond breaking.

Light absorption may be associated either with the creation of electron–hole pairs in the near-surface region of the solid, with the excitation of bonds within the adsorbed molecule (which are not directly involved in the bond formation with the surface), or with direct excitation of the surface–adsorbate bond. Depending on whether relaxation of the excitation to (at least local) thermal equilibrium precedes the chemical transformation or not, classification into thermal or non-thermal processes can be made. Attempts for distinction can be based on comparison with results to be expected for true thermal origin of the corresponding process.

With the UV-laser-induced desorption of NO from a NiO surface investigated here, at least part of these molecules is of non-thermal origin. The evidence is essentially based on the strong dependence of the desorption cross section on the binding state of the adsorbate, and (more directly) on the energy distributions of the desorbing particles.

For thermal desorption the yield is primarily governed by the temperature rise associated with the irradiation. If we assume for the moment that the temperature jump is large enough to cause – starting from 140 K – thermal desorption of the NO–NiO species with its TDS maximum at 220 K, then also the species chemisorbed on Ni(100) and exhibiting its TDS peak around 350 K should desorb if the base temperature is 300 K. (Unless the optical and thermal properties of the substrate are so strongly dependent on temperature that the temperature rise with constant laser power is much smaller at 300 K than at 140 K, for which, however, no evidence was found.) However, no detectable amounts of NO were observed to come off the surface under the latter conditions. On the other hand, the cross section for desorption via electronic excitation is much more efficiently quenched with metallic substrates than with non-metals exhibiting band gaps. This statement is based on general experience with electron-stimulated desorption (ESD) and related processes [34] and makes it plausible why the desorption cross section for the NO–NiO system far exceeds that for the NO–Ni system. From the results reported by Buntin et al. [12c] for UV photodesorption of NO from metallic Pt(111) it can be estimated that in this case the cross section is at least two orders of magnitude smaller than in the present system which corroborates this conclusion.

Furthermore, for a thermal desorption process the yield would never decrease with increasing coverage, as observed here, but would rather exhibit a tendency for a more-than-linear increase, since the adsorption energy and hence the desorption temperature in general decrease. On the other hand, such an effect is well known in ESD experiments [34]: Orbital interactions between the adsorbed species at high coverages leading to electronic band formation open up additional channels for delocalization and hence relaxation of the electronic excitation energy, and thereby the cross section for desorption drops.

Even more direct evidence for the non-thermal origin of desorbing molecules arises from the measured energy distributions. Already the observed bimodal time-of-flight distributions would require rather artificial assumptions for explanation on the basis of thermal excitation. Unless desorption proceeds over an energy barrier, the temperature equivalent to the energy content of any degree of freedom of the desorbing molecules may never exceed the surface temperature if desorption is of thermal origin. Such a barrier – if existent – must manifest itself also as an activation energy for the reverse process of adsorption. Since the sticking coefficient for NO on the NiO surface kept at 140 K is fairly high (determined to be about 0.6), such a possibility can clearly be ruled out. Values of  $\langle E_{\text{trans}} \rangle / 2k > 2000$  K as derived for the “fast” particles of the TOF distributions are certainly far outside any surface temperatures which might be reached by the laser irradiation, and therefore their origin is clearly non-thermal.

The situation is less clear for the fraction of “slow” particles. Their mean translational energy of  $330 \pm 50$  K is higher than the maximum values estimated for the surface temperature, however, this estimate ( $\sim 170$  K) was rough and also in view of the large error bars of  $\langle E_{\text{trans}} \rangle$  a thermal nature of the “slow” molecules cannot definitely be ruled out. Their rotational temperature of 150 K, as well as their absence in the  $v'' = 1$  state, could well be reconciled with a thermal nature.

Bimodal time-of-flight distributions of molecules desorbed by laser pulses have also been observed with several other systems: In experiments by Natzle et al. [17] with thick condensed NO layers under similar conditions as in the present work, “slow” particles with translational temperatures between 160 and 280 K were clearly identified as thermal in origin. UV/Vis laser-induced desorption in the system NO–Pt(poly) [12a,b] as well as NO–Pt(111) [12c] revealed again bimodal TOF distributions from which the “slow” part was identified with thermal origin. Although there exist some inconsistencies with such an interpretation of the present data, we tend to favour again this assignment and shall therefore focus the further discussion on the “fast” particles which are clearly of non-thermal origin.

We believe that the most appropriate model to describe the “fast” particle desorption starts with excitation to a repulsive region of an electronically excited state potential of the surface–adsorbate system as depicted schematically in fig. 14, curve (b), as a consequence of a transition from the ground state (curve (a)) initiated by absorption of a UV photon. Relaxation of the excitation energy in the various degrees of freedom will compete with the desorption process and thus lead to the final energy distributions of the gaseous molecules. The electronic excitation of the surface–adsorbate bond may in principle occur in different ways:

(1) Indirectly, via excitation of the solid. Electron energy loss spectroscopy (EELS) from NiO exhibits absorption bands in the energy range of the laser

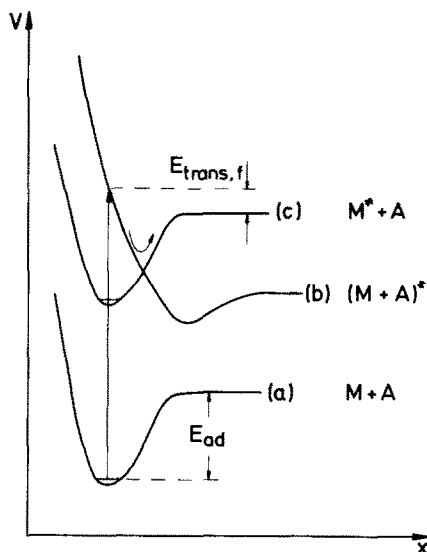


Fig. 14. Schematic one-dimensional surface(M)-adsorbate(A) interaction potentials. Curve (a): Electronic ground state. Curve (b) marks the electronically excited  $(M+A)^*$  complex to which a transition occurs (either directly or indirectly) by photon absorption. Curve (c) is the ground-state potential (a) vertically displaced by an energy equivalent to the value transferred to the solid by relaxation. As a consequence of total energy balance the particle escapes from the surface with a kinetic energy  $E_{\text{trans},f}$ . Adopted from Gomer [44] treating electron-stimulated desorption.

radiation applied (5.0–6.4 eV) with maxima at 4.6 and 6.9 eV, probably reflecting the creation of  $O^2 2p \rightarrow Ni^{2+} 3d$  charge transfer excitons [36]. These might then diffuse to the surface and interact with the adsorbate through its partly unoccupied  $2\pi$ -levels, giving rise to excitation of the substrate-adsorbate bond of the type illustrated by fig. 14. Such a mechanism was recently proposed for photodesorption of NO from a Pt(111) surface [12b] as well as for the NO-Si system [10c].

(ii) Directly, through excitation of the adsorbate. While in the quoted work on NO/Si [10c] conclusive evidence for primary excitation of the solid was deduced from the wavelength dependency of the desorption yield, the alternate possibility of direct optical excitation of the adsorbed molecule cannot a priori be ruled out. The system NO/Ni (not NiO!) exhibits a broad EELS band centred at 5.6 eV which was attributed to an excitation of the  $2\pi$ -derived level of the adsorbed NO [28]. Likewise, in previous work [37] a peak at 4.8 eV had been interpreted as being caused by a transition from the  $2\pi$ -level to a state which is antibonding with respect to the Ni-NO bond.

Irrespective of the nature of the dominant mode of primary excitation, which cannot be decided on the basis of the available experimental material, desorption starts from a state of the type depicted as curve (b) in fig. 14, and

the nature of this state will certainly be of importance for the resulting energy distributions of the molecules after release into the gas phase. In electron-stimulated desorption (ESD) experiments with NO/Pt(111) Burns et al. [38] observed a threshold near electron energies of 6 eV, while the desorbing molecules exhibited a peak translational energy around 50 meV – these data are similar to those for the present photodesorption results, so that it is suggested that desorption starts in both types of experiments from the same type of excited state. The authors of ref. [38] propose a quite interesting picture about the nature of the electronically excited species: The excitation consists in creation of a hole in the NO 5s level which is rapidly screened by the substrate electrons whereby the occupancy of the  $2\pi$ -level is increased. In this way the excited species becomes O<sub>2</sub>-like which is weakly held at the surface and prefers an orientation of its molecular axis parallel to the surface instead of the vertical orientation of (ground-state) NO. Calculations of the time evolution of a system excited from an initial state with fixed orientation of the molecular axis (= chemisorbed NO) into a long-lived state of a free rotor in a weak Morse potential with a shifted equilibrium position from the surface (= adsorbate complex after electronic excitation) yields translational and rotational energy distributions of the desorbing particles which are in qualitative good agreement with the experimental findings. It is felt that this model might also serve for explanation of the present results:

The observed *increase* of the translational energy with rotational energy as evidenced by fig. 6 (i.e. the faster a molecule rotates the faster it comes off the surface) seems to be characteristic for desorption processes starting from a repulsive potential: this effect was also observed with other systems undergoing photodesorption [12], as well as with the formation of NO by decomposition of NO<sub>2</sub> at a Ge surface [39]. In the latter case the reaction NO<sub>2</sub> + Ge → Ge–O + NO is strongly exothermic and NO is released into the gas phase on a downhill trajectory along the reaction coordinate. In the case of thermal desorption from the ground-state attractive potential, on the other hand, the translational energy is generally found to be independent of  $E_{\text{int}}$  [39]. Finally, in the case of direct-inelastic surface scattering of molecules which were initially rotationally cold, the resulting mean translational energy *decreases* with  $E_{\text{rot}}$  [22] – an effect which may be explained on the basis of rather simple models [40]. Interpretation of the observed increase of the translational energy with internal energy as well as of the influence of the spin–orbit level on  $\langle E_{\text{trans}} \rangle$  (as evidenced by fig. 6) is still awaiting theoretical analysis.

The most striking manifestation of the non-thermal origin of the desorbing “fast” particles stems from the observed spin–orbit selectivity. We recall the results shown in fig. 9 whereafter desorption with  $h\nu = 6.4$  eV yields at low  $J''$  predominantly particles in the  ${}^2\Pi_{1/2}$  state, while at higher rotational energies both spin–orbit levels become equally populated. Such an effect had never been reported for systems either undergoing thermal desorption or direct-in-

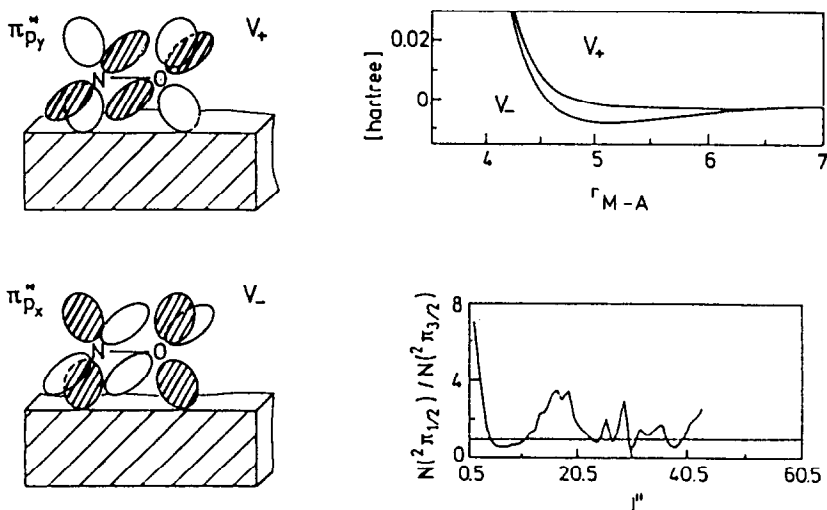


Fig. 15. Interaction potentials  $V_+$  and  $V_-$  for a NO molecule oriented parallel to a surface with either the  $2\pi_{p_y}^*$  or  $2\pi_{p_x}^*$  orbital being singly occupied. The calculated population ratio  $R_N = N(2^2\Pi_{1/2})/N(2^2\Pi_{3/2})$  for molecules scattered at these potentials exhibits a pronounced increase at low  $J''$  values, in qualitative agreement with the experimental results shown in fig. 10. After Smedley et al. [41].

elastic scattering, although an experimental study belonging in the latter category [33] prompted the development of a full-fledged quantum-mechanical theory for *scattering* of NO at a surface [41], the conclusions of which will be used for interpretation of the present findings.

The  $2\pi$ -orbital of NO is singly occupied. If the axis of this molecule is parallel to the surface, there will exist two interaction potentials with the surface,  $V_+$  and  $V_-$ , depending on whether the singly occupied  $2\pi$ -orbital is oriented parallel or perpendicular to the surface plane (fig. 15). If the molecule is oriented perpendicular to the surface – which can be assumed to be the stable ground-state geometry – these two potentials will of course be degenerate. According to the theory by Smedley et al. [41], the existence of these two types of potentials will lead to non-equal populations of the two spin-orbit manifolds after scattering of NO at a rigid and flat surface. For the type of potentials  $V_+$  and  $V_-$  reproduced in fig. 15c, the calculated population ratio  $N(2^2\Pi_{1/2})/N(2^2\Pi_{3/2})$  shows high values (corresponding to marked underpopulation of  $2^2\Pi_{3/2}$ ) at low  $J''$  values, while it rapidly levels off with increasing  $J''$  (possibly exhibiting additional weak maxima at intermediate values which most probably would be within the experimental scatter of our data). The equal population of both spin-orbit manifolds at higher final rotational energy is due to a quantum-mechanical interference effect between the wave

functions belonging to the two potentials  $V_+$  and  $V_-$  which increases with increasing  $J''$ .

The sketched ideas may be adopted to the present case of photodesorption if this is considered to represent a half-collision in which the system starts to leave the surface from a point of the repulsive part of the interaction potential. If we assume that this process starts from the geometry of the ground state with the molecular axis normal to the surface, the potentials  $V_+$  and  $V_-$  would of course be identical and no spin-orbit selectivity would be expected. According to the quoted model by Burns et al. [38], however, desorption starts from an excited state representing nearly a free rotator. These calculations revealed in addition that those molecules de-exciting into the ground-state from orientations near the surface normal have a higher probability for being retrapped than those which reached larger angles during the lifetime of the electronically excited state. As a consequence it is to be expected that a large fraction of the desorbing molecules originates indeed from configurations in which their molecular axis was inclined towards the surface plane so that the degeneracy of the potentials  $V_+$  and  $V_-$  is lifted and the spin-orbit selectivity may occur.

Unequal spin-level occupations have also been reported for NO formed by photodissociation of several gaseous molecules [42,43]. In a most recent study on the photodecomposition of  $\text{CH}_2\text{ONO}$  the following conclusion was reached [43]: "The mechanism which channels population into the  $\Pi_{1/2}$  and  $\Pi_{3/2}$  states is expected to be quite complex, since it involves the geometry along the reaction path and the electronic structures of the parent and the fragments." This statement certainly also holds for the present example, and it is felt that understanding of this aspect of photodesorption is not so far behind the present state of knowledge in gas-phase photochemistry.

After having demonstrated that the molecules desorbing in the "fast" channel are of non-thermal origin as reflected by their energy distributions, it has to be pointed out that the excitation energy has nevertheless been transmitted predominantly to the solid. This becomes evident from inspection of fig. 16 which shows the total energy balance for  $v'' = 0$  particles desorbing in the  $^2\Pi_{1/2}$  (a) and  $^2\Pi_{3/2}$  (b) spin-orbit manifold, respectively. These plots show how the total energy  $E_t$  of the desorbing molecules varies with their rotational energy. Even the very few particles exhibiting the highest rotational energies carry off less than about 0.6 eV total energy. From the TDS peak temperature of 220 K we estimate the binding energy with the surface to be also of the order of 0.6 eV, so that from the available photon energy of 6.4 eV at least 5.2 eV or 80% are in any case transferred to the heat bath of the solid. (This percentage is – if averaged over all desorbing particles – still substantially higher since their *mean* energy content is of course much smaller.) It has to be concluded that the excited  $(M + A)^*$  surface complex as characterized schematically by the potential curve (b) of fig. 14 relaxes into a  $(M^* + A)$  state

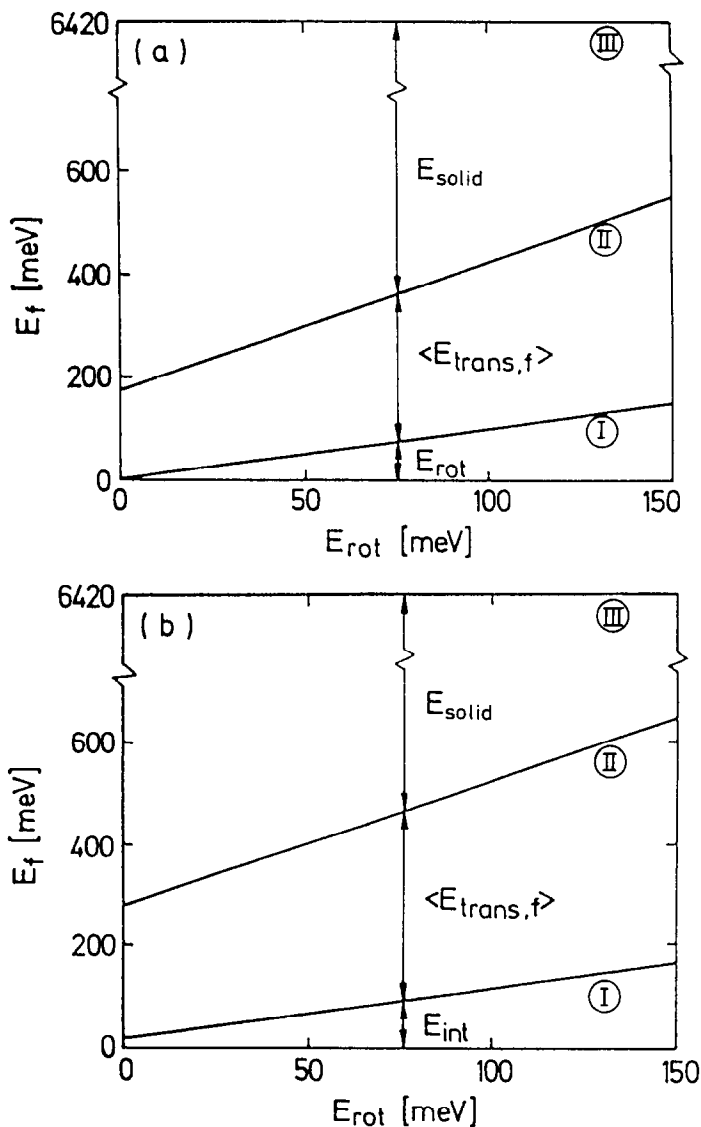


Fig. 16. Energy balance for photodesorption of NO, assuming a single photon process as primary step. The difference between the photon energy  $E_{rot} = 6.42$  eV and the internal and translation energies,  $E_{int}$  and  $\langle E_{trans,f} \rangle$ , of the desorbing particles is transferred to the solid,  $E_{surface}$  ( $v'' = 0$ ): (a)  $^2\Pi_{1/2}$  manifold, (b)  $^2\Pi_{3/2}$  manifold.

as illustrated by curve (c) in this figure. (Since the NO molecules probed by the LIF technique are in their electronic ground state, such a radiationless relaxation process must have necessarily occurred during the desorption

process. If we would assume that a substantial fraction of the NO desorbs in the electronically excited state, followed by fluorescence in the gas phase, then their distribution would reflect the Franck–Condon factors for this decay and a much larger population of  $v'' = 1$  than the observed 1% would occur.) This model has been adopted from electron-stimulated desorption according to the MGR model [44]. Depending on the separation  $x$  between the surface and the adsorbate at which this relaxation takes place, the desorbing molecule will carry off more or less excess translational energy. If  $x$  is smaller than a critical distance, the gain in kinetic energy will not be sufficient to overcome the attractive ground-state potential and the particle will be recaptured by the surface. In this way it becomes quite obvious that the nature of the electronic coupling and therefore the adsorption state is a very sensitive parameter influencing the cross section for photodesorption, but as mentioned, these are well-established concepts of ESD. A natural extension would consist in including also the rotational degrees of freedom into this consideration which might finally explain why molecules desorbing with higher rotational energies exhibit also higher mean translational energies.

## 5. Conclusions

Transformation of a Ni(100) surface into a NiO overlayer (either by thermal oxidation in O<sub>2</sub> or by photodecomposition of adsorbed NO<sub>2</sub>) leads to the creation of a low-temperature state of adsorbed NO, from which it desorbs thermally around 220 K, as well as by excitation with UV photons ( $h\nu = 5.0$  and 6.4 eV, respectively). The photodesorption cross section of about  $2 \times 10^{-17}$  cm<sup>2</sup> is orders of magnitude larger than that for NO adsorbed on a metallic substrate which has to be attributed to the reduced probability for electronic de-excitation at the NiO surface exhibiting a band gap.

Fully state-resolved measurements on the energy distributions of the various degrees of freedom (translational, rotational, vibrational, spin–orbit splitting) of the desorbing molecules reveal clear evidence that at least part of them is of non-thermal origin:

- (a) The translational energy distributions are bimodal. The average kinetic energy of the “fast” particles increases with increasing internal energy and may reach values equivalent to  $\sim 3000$  K.
- (b) The rotational state populations depend on the spin–orbit manifold under consideration and are strongly non-Boltzmann for the  ${}^2\Pi_{3/2}$  level. The average rotational energy does not reach the high values of  $\langle E_{\text{trans}} \rangle$ , but again exceeds the surface temperature substantially.
- (c) The population of the  $v' = 1$  state of about 1% was found to be smaller than in a previous preliminary study [19], but is still considerably larger than the value corresponding to thermal equilibrium with the solid.

(d) The most pronounced effect is observed with respect to the populations  $N(^2\Pi_{1/2})$  and  $N(^2\Pi_{3/2})$  of the two spin-orbit manifolds: For low rotational quantum numbers their ratio may reach values of up to 40.

Qualitative account of the observed phenomena is obtained by adopting the concepts developed for electron-stimulated desorption (MGR mechanism): The electron-hole pairs created in the near-surface region by photon absorption cause transition of the adsorbate-substrate system into the repulsive potential of an excited state from where dissociation (= desorption) competes with relaxation into the ground state. The observed higher yields for photodesorption from a semiconducting (NiO) with respect to a metallic (Ni) surface, as well as of the *decrease* of the yield with increasing coverage are manifestations of the changing effectiveness of these relaxation channels. The pronounced spin-orbit selectivity is tentatively interpreted in terms of a quantum-mechanical interference effect as treated theoretically by Smedley et al. [41].

The field of the dynamics of photochemical processes at surfaces is certainly only at its beginnings, and certainly much more experimental and theoretical experience has to be accumulated before detailed understanding can be expected.

## Acknowledgements

The authors are indebted to Dr. E. Hasselbrink for stimulating discussions and critical reading of the manuscript. Financial support by the Studienstiftung des Deutschen Volkes (F.B.) and by the A. von Humboldt-Stiftung (A.V.H.) is gratefully acknowledged.

## References

- [1] T.J. Chuang, *Surface Sci. Rept.* 3 (1983) 1.
- [2] D. Bäuerle, Ed., *Laser Processing and Diagnostics*, Vol. 39 of Springer Series in Chemical Physics (Springer, Berlin, 1984).
- [3] D.J. Ehrlich and J.Y. Tsao, *J. Vacuum Sci. Technol. B* 1 (1983) 969.
- [4] (a) R.M. Osgood, *Ann. Rev. Phys. Chem.* 34 (1983) 77;  
(b) R.M. Osgood and T.F. Deutsch, *Science* 227 (1985) 709.
- [5] G.S. Selwyn and M.C. Lin, in: *Lasers as Reactants and Probes in Chemistry*, Eds. W.M. Jackson and A.B. Harvey (Howard University Press, Washington, DC, 1985).
- [6] (a) Desorption Induced by Electronic Transitions, DIET I, Eds. N.H. Tolk, M.M. Traum, J.C. Tully and T.E. Madey, Vol. 24 of Springer Series in Chemical Physics (Springer, Berlin, 1983);  
(b) Desorption Induced by Electronic Transitions, DIET II, Eds. W. Brenig and D. Menzel, Vol. 4 of Springer Series in Surface Sciences (Springer, Berlin, 1985).

- [7] (a) V.S. Letokhov, V.G. Movshev and S.V. Chekalin, *Soviet Phys.-JETP* 54 (1981) 257;  
(b) V.S. Antonov, V.S. Letokhov and A.N. Shibabov, *Appl. Phys.* 25 (1981) 71.
- [8] N. Nishi, H. Shinohara and T. Okuyama, *J. Chem. Phys.* 80 (1984) 3898.
- [9] (a) E.B.D. Bourdon, J.P. Cowin, I. Harrison, J.C. Polanyi, J. Segner, C.D. Stanners and P.A. Young, *J. Phys. Chem.* 88 (1984) 6100;  
(b) E.B.D. Bourdon, P. Das, I. Harrison, J.C. Polanyi, J. Segner, C.D. Stanners, R.J. Williams and P.A. Young, *Faraday Disc. Chem. Soc.* 82 (1986) 343;  
(c) St. J. Dixon-Warren, I. Harrison, K. Leggett, M.S. Matyjaszczyk, J.C. Polanyi and P.A. Young, *J. Chem. Phys.* 88 (1988) 4092.
- [10] (a) C.E. Bartosch, N.S. Gluck, W. Ho and Z. Ying, *Phys. Rev. Letters* 57 (1986) 1425;  
(b) N.S. Gluck, Z. Ying, C.E. Bartosch and W. Ho, *J. Chem. Phys.* 87 (1987) 4957;  
(c) Z. Ying and W. Ho, *Phys. Rev. Letters* 60 (1988) 57;  
(d) T.A. Germer and W. Ho, *J. Chem. Phys.* 89 (1988) 562;  
(e) Z. Ying and W. Ho, *J. Vacuum Sci. Technol. A* 6 (1988) 834.
- [11] J.R. Creighton, *J. Appl. Phys.* 59 (1986) 410.
- [12] (a) D. Burgess, Jr., D.A. Mantell, R.R. Cavanagh and D.S. King, *J. Chem. Phys.* 85 (1986) 3123;  
(b) D. Burgess, Jr., R.R. Cavanagh and D.S. King, *J. Chem. Phys.* 88 (1988) 6556;  
(c) S.A. Buntin, L.J. Richter, R.R. Cavanagh and D.S. King, *Phys. Rev. Letters* 61 (1988) 1321.
- [13] K. Dömen and T.J. Chuang, *Phys. Rev. Letters* 59 (1987) 1484.
- [14] (a) F.L. Tabares, E.P. Marsh, G.A. Bavch and J.P. Cowin, *J. Chem. Phys.* 86 (1987) 738;  
(b) E.P. Marsh, M.R. Schneider, T.L. Gilton, F.L. Tabares, W. Meier and J.P. Cowin, *Phys. Rev. Letters* 60 (1988) 2551.
- [15] F.G. Celii, P.M. Whitmore and K.C. Janda, *Chem. Phys. Letters* 138 (1987) 257.
- [16] W. Hoheisel, K. Jungmann, M. Vollmer, R. Weidenauer and F. Träger, *Phys. Rev. Letters* 60 (1988) 1649.
- [17] W.C. Natzle, D. Padowitz and S.J. Sibener, *J. Chem. Phys.* 88 (1988) 7975.
- [18] V.H. Grassian and G.C. Pimentel, *J. Chem. Phys.* 88 (1988) 4484.
- [19] D. Weide, P. Andresen and H.-J. Freund, *Chem. Phys. Letters* 136 (1987) 107.
- [20] F. Budde, A.V. Hamza, P.M. Ferm, G. Ertl, D. Weide, P. Andresen and H.-J. Freund, *Phys. Rev. Letters* 60 (1988) 1518.
- [21] (a) J.A. Barker and D.J. Auerbach, *Surface Sci. Rept.* 4 (1984) 1;  
(b) C.T. Rettner and D.J. Auerbach, *Comments At. Mol. Phys.* 20 (1987) 153;  
(c) M.P. D'Evelyn and R.J. Madix, *Surface Sci. Rept.* 4 (1984) 1;  
(d) M.C. Lin and G. Ertl, *Ann. Rev. Phys. Chem.* 37 (1986) 587.
- [22] A. Mödl, T. Gritsch, F. Budde T.J. Chuang and G. Ertl, *Phys. Rev. Letters* 57 (1986) 384.
- [23] B.E. Koel, D.E. Peebles and J.M. White, *Surface Sci.* 125 (1983) 709.
- [24] J.H. Bechtel, *J. Appl. Phys.* 46 (1975) 1586.
- [25] F. Budde, T. Gritsch, A. Mödl, T.J. Chuang and G. Ertl, *Surface Sci.* 178 (1986) 798.
- [26] M.S. Chou, A.M. Dean and E. Stern, *J. Chem. Phys.* 78 (1983) 5962.
- [27] R. Engleman, Jr. and P.E. Rouse, *J. Mol. Spectrosc.* 37 (1971) 240.
- [28] D.E. Peebles, E.L. Hardegree and J.M. White, *Surface Sci.* 148 (1984) 635.
- [29] (a) P.H. Holloway and J.B. Hudson, *Surface Sci.* 43 (1974) 123, 141;  
(b) H. Conrad, G. Ertl, J. Küppers and E.E. Latta, *Solid State Commun.* 17 (1975) 497.
- [30] (a) G. Odörfer, H. Geisler, R. Jaeger, H. Kühlenbeck and H.-J. Freund, to be published;  
(b) G. Odörfer, G. Watson, K.-D. Tsuei, E.W. Plummer and H.-J. Freund, to be published.
- [31] E. Hasselbrink, S. Jakubith, M. Wolf and G. Ertl, in preparation.
- [32] (a) E. Escalona Platero, S. Coluccia and A. Zecchina, *Langmuir* 1 (1985) 407;  
(b) E. Escalona Platero, B. Fubini and A. Zecchina, *Surface Sci.* 179 (1987) 404.
- [33] (a) J.P. Cowin, D.J. Auerbach, C. Becker and L. Wharton, *Surface Sci.* 78 (1978) 545;  
(b) J.P. Cowin, *Phys. Rev. Letters* 54 (1985) 368.

- [34] (a) D. Menzel, Nucl. Instr. Methods B 13 (1986) 507;  
(b) D. Menzel, in: Study of Surfaces and Interfaces by Electron Optical Techniques, Eds. A. Howie and U. Valdré (Plenum, New York, 1988).
- [35] A.C. Luntz, A.W. Kleyn and D.J. Auerbach, J. Chem. Phys. 76 (1982) 737.
- [36] K. Akimoto, Y. Sakisaka, M. Nishijima and M. Onchi, J. Phys. C 11 (1987) 2535.
- [37] Y. Sakisaka, M. Miyamura, J. Tamaki, M. Nishijima and M. Onchi, Surface Sci. 93 (1986) 327.
- [38] A.R. Burns, E.B. Stechel and D.R. Jennison, Phys. Rev. Letters 58 (1987) 250.
- [39] F. Budde, A. Mödl, A.V. Hamza, P.M. Ferm and G. Ertl, Surface Sci. 192 (1987) 507.
- [40] (a) J. Kimman, C.T. Rettner, F. Fabre, D.J. Auerbach, J.A. Baker and J.C. Tully, Phys. Rev. Letters 57 (1986) 2053;  
(b) T. Brunner, R. Brako and W. Brenig, Phys. Rev. A 35 (1987) 5266.
- [41] J. Smedley, G.C. Corey and M.H. Alexander, J. Chem. Phys. 87 (1987) 3128.
- [42] (a) F. Lahmani, L. Lardeux and D. Solgadi, Chem. Phys. Letters 129 (1986) 24;  
(b) M. Noble, C.X.W. Qian, H. Reislser and C. Witting, J. Chem. Phys. 85 (1986) 5763;  
(c) M.R.S. McCoustra and J. Pfab, Chem. Phys. Letters 137 (1987) 355.
- [43] U. Brühlmann and J.R. Huber, Chem. Phys. Letters 143 (1988) 199.
- [44] R. Gomer in ref. [6a], p. 40.